Journal of Solid State Chemistry 184 (2011) 1346–1352

Contents lists available at ScienceDirect

Journal of Solid State Chemistry

journal homepage: www.elsevier.com/locate/jssc

# Mechanochemical–thermal preparation and structural studies of mullite-type $Bi_2(Ga_xAl_{1-x})_4O_9$ solid solutions

K.L. Da Silva [a,b,c], V. Šepelák [d,*,1], A. Düvel [b], A. Paesano Jr. [c], H. Hahn [d], F.J. Litterst [e], P. Heitjans [b], K.D. Becker [a]

[a] Institute of Physical and Theoretical Chemistry, Technische Universität Braunschweig, Hans-Sommer-Str. 10, 38106 Braunschweig, Germany
[b] Institute of Physical Chemistry and Electrochemistry, Leibniz University Hannover, Callinstr. 3a, 30167 Hannover, Germany
[c] Department of Physics, State University of Maringá, Av. Colombo 5790, 87020-900 Maringá, Brazil
[d] Institute of Nanotechnology, Karlsruhe Institute of Technology, Hermann-von-Helmholtz-Platz 1, 76344 Eggenstein-Leopoldshafen, Germany
[e] Institute of Condensed Matter Physics, Technische Universität Braunschweig, Mendelssohnstr. 3, 38106 Braunschweig, Germany

ARTICLE INFO

*Article history:*
Received 28 December 2010
Received in revised form
11 March 2011
Accepted 4 April 2011
Available online 13 April 2011

*Keywords:*
Mullite
Mechanochemical processing
Cation distribution
Rietveld refinement
NMR

ABSTRACT

A series of $Bi_2(Ga_xAl_{1-x})_4O_9$ solid solutions ($0 \le x \le 1$), prepared by mechanochemical processing of $Bi_2O_3/Ga_2O_3/Al_2O_3$ mixtures and subsequent annealing, was investigated by XRD, EDX, and $^{27}$Al MAS NMR. The structure of the $Bi_2(Ga_xAl_{1-x})_4O_9$ solid solutions is found to be orthorhombic, space group *Pbam* (No. 55). The lattice parameters of the $Bi_2(Ga_xAl_{1-x})_4O_9$ series increase linearly with increasing gallium content. Rietveld refinement of the XRD data as well as the analysis of the $^{27}$Al MAS NMR spectra show a preference of gallium cations for the tetrahedral sites in $Bi_2(Ga_xAl_{1-x})_4O_9$. As a consequence, this leads to a far from random distribution of Al and Ga cations across the whole series of solid solutions.



## 1. Introduction

Bismuth-bearing oxides $Bi_2M_4O_9$ ($M$=$Fe^{3+}$, $Ga^{3+}$, $Al^{3+}$ and $In^{3+}$), their substituted derivates $Bi_{2-2x}A_{2x}M_4O_{9-x}$ (e.g. $A$=$Sr^{2+}$), and the wide variety of respective solid solutions are members of the mullite-type family of crystal structures [1–5]. In $Bi_2M_4O_9$, sites for $M^{3+}$ ions of tetrahedral ($T$) and octahedral [$O$] coordination occur in equal numbers with $N_{(T)}=N_{[O]}=2$, where $N_{(T)}$ and $N_{[O]}$ are the numbers of the indicated non-equivalent sites per formula unit of the mullite-type material. The crystal structure of $Bi_2M_4O_9$ is shown in Fig. 1. It is characterized by columns of edge-sharing $MO_6$ octahedra parallel to the $c$-axis which are interconnected by $M_2O_7$ double tetrahedra ($M$=Ga or Al).

The ($T$) and [$O$] sites for $M^{3+}$ ions can accept both transition and main group metal cations. As a consequence, many materials properties depend on the distribution of different $M^{3+}$ cations on the two non-equivalent coordination sites. Some of these materials show remarkable ionic conductivity of anions [5,6] having potential as electrolytes in solid oxide fuel cells or as oxygen sensors [7,8]. Others possess a high emissivity in the infrared region and, thus, may be utilized as high-energy scintillator materials [9,10]. Another point of fundamental interest in these materials is related to the role played by the lone electron pair of $Bi^{3+}$ ions with respect to structure and materials properties of this class of compounds [2].

In the present work, the synthesis of $Bi_2(Ga_xAl_{1-x})_4O_9$ solid solutions ($0 \le \times \le 1$) of the mullite-type is reported via mechanochemical processing of stoichiometric $Bi_2O_3/Ga_2O_3/Al_2O_3$ mixtures and subsequent annealing. It should be emphasized that, whereas the end members $Bi_2Ga_4O_9$ and $Bi_2Al_4O_9$ of the series are treated to a limited extent in the literature [2,7,10–12], the preparation of the complex $Bi_2(Ga_xAl_{1-x})_4O_9$ mixed crystals ($0 < x < 1$) has only very recently been reported using the glycerine method for synthesis [13,14]. The combined mechanochemical/thermal process used in the present study represents a simple, less elaborate, high-yield, shorter processing time, and, thus, a low-cost procedure for the synthesis of these structurally and constitutionally complex materials. On the basis of the Rietveld analysis of the X-ray diffraction (XRD) data, the unit cell dimensions and the cation occupation factors in the investigated systems are determined. In addition to the XRD analysis, quantitative information on the distribution of aluminium ions in the mixed crystals is obtained employing $^{27}$Al magic angle spinning (MAS) nuclear magnetic resonance (NMR) spectroscopy.

* Corresponding author. Fax: +49 721 60826368.
*E-mail address:* vladimir.sepelak@kit.edu (V. Šepelák).
[1] On leave from the Slovak Academy of Sciences, Watsonova 45, Košice, Slovakia.

0022-4596/$ - see front matter © 2011 Elsevier Inc. All rights reserved.
doi:10.1016/j.jssc.2011.04.007

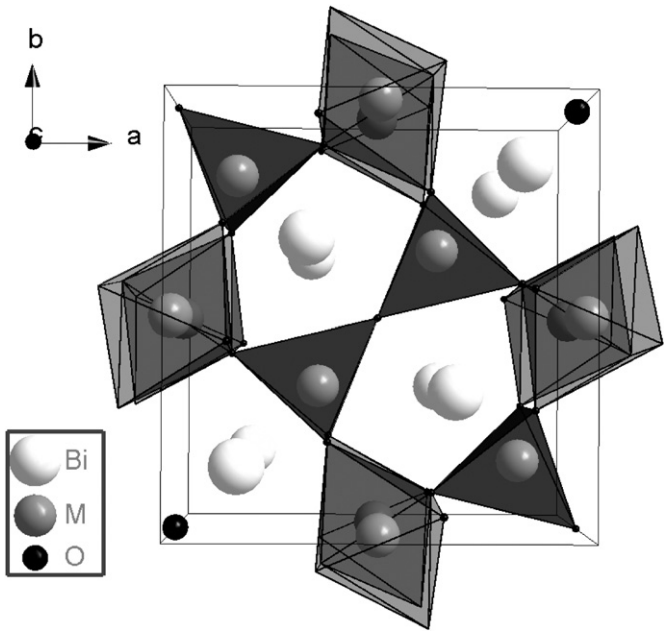


**Fig. 1.** Crystal structure of $Bi_2M_4O_9$ (space group *Pbam*) is characterized by chains of edge-connected $MO_6$ octahedra along the *c*-axis which are interconnected by $M_2O_7$ double tetrahedra.

## 2. Experimental

Polycrystalline $Bi_2(Ga_xAl_{1-x})_4O_9$ solid solutions in the range $0 \le x \le 1$ were prepared from mixtures of $Bi_2O_3$ (Alfa Aesar, 99.999%), $Ga_2O_3$ (Alfa Aesar, 99.99%), and $\alpha$-$Al_2O_3$ (Aldrich, 99.998%) by a combined mechanochemical/thermal synthesis method using a high-energy planetary ball mill (Pulverisette 6, Fritsch). The starting materials were weighted in stoichiometric amounts and milled in a chamber (250 $cm^3$ in volume) with 22 balls (10 mm in diameter) made of tungsten carbide. The ball-to-powder weight ratio was 22:1. The powders were milled for 3 h at 600 rpm in air. After this procedure, the as-milled materials were annealed at 800 °C in air for 24 h.

The XRD data of the $Bi_2(Ga_xAl_{1-x})_4O_9$ ($0 \le x \le 1$) mixed crystals were collected using a PW 1820 X-ray diffractometer (Philips, Netherlands), operating in Bragg configuration and using Cu-$K\alpha$ radiation. X-ray powder diffraction step scans were taken from 10° to 60° $2\theta$, using a step size of 0.02° $2\theta$ and a data collection time of 5 s per step. The Rietveld refinements of the XRD data were performed using a full-profile analysis program [15].

$^{27}$Al MAS NMR spectra were taken at room temperature using a Bruker MSL 400 NMR spectrometer equipped with an Oxford cryomagnet of a nominal magnetic field of 9.4 T. The $^{27}$Al NMR resonance frequency was 104.229 MHz. The samples were rotated in 4 mm rotors made of boron nitride at a spinning frequency of 10 kHz. A single pulse sequence with a pulse length of 1 μs was used for recording. Typically 512 scans were acquired with a recycle delay of 2 s. The spectra were referenced to an aqueous solution of $Al(NO_3)_3$. The fraction of aluminium ions located on octahedral sites, $\lambda(Al_{[O]}) = N(Al_{[O]})/(N(Al_{(T)}) + N(Al_{[O]}))$, in the $Bi_2(Ga_xAl_{1-x})_4O_9$ mixed crystals was calculated from the spectra according to $\lambda(Al_{[O]}) = A(Al_{[O]})/(A(Al_{(T)}) + A(Al_{[O]}))$, where $A(Al_{(T)})$ and $A(Al_{[O]})$ are the $^{27}$Al NMR subspectral areas due to tetrahedrally and octahedrally coordinated aluminium ions, respectively, and where $N(Al_{(T)})$ and $N(Al_{[O]})$ denote the corresponding number of cations per formula unit of $Bi_2(Ga_xAl_{1-x})_4O_9$.

## 3. Results and discussion

It was revealed that, independently of different stoichiometric amounts of the starting simple oxides ($Bi_2O_3$, $Ga_2O_3$, and $Al_2O_3$) used for the synthesis of $Bi_2(Ga_xAl_{1-x})_4O_9$ solid solutions, the mechanochemical processing of $Bi_2O_3/Ga_2O_3/Al_2O_3$ mixtures for milling times up to 3 h does not lead to the formation (mechanosynthesis) of a new phase. With increasing milling time, X-ray diffraction merely revealed a decrease in the intensity and a broadening of the Bragg peaks of the individual simple oxides (XRD patterns are not shown), reflecting the reduction of their crystallite size and the accumulation of strains in their structure. The average crystallite size of the starting oxides, typically in a micrometre range, was reduced to about 30 nm after 3 h of milling. The XRD patterns of the selected as-milled mixtures followed by their annealing at 800 °C in air for 24 h are shown in Fig. 2a. As clearly seen, the combined mechanochemical/thermal treatment used here leads to the formation of $Bi_2(Ga_xAl_{1-x})_4O_9$ solid solutions ($0 \le x \le 1$); all the diffraction peaks correspond to the orthorhombic mullite-type phase with space group *Pbam* (No. 55).

It should be emphasized that the combined mechanochemical/thermal process used in the present study represents a simple, less elaborate, high-yield, shorter processing time, and, thus, a low-cost procedure for the synthesis of $Bi_2M_4O_9$-type compounds. In this context, it should be noted that various methods have been described for the synthesis of polycrystalline $Bi_2M_4O_9$-type compounds. For example, Giaquinta et al. [3,4] annealed stoichiometric amounts of oxides ($Bi_2O_3$, $M_2O_3$; $M$=Fe, Ga [3] and Fe, Al [4]) at 850 °C in air for two weeks with frequent grindings. Recently, Voll et al. [16] applied the glycerin method for the synthesis of $Bi_2(Fe_xAl_{1-x})_4O_9$ mixed crystals using temperatures up to 850 °C. This method has also been used by Debnath et al. [13,14] in their recent synthesis of $Bi_2(Ga_xAl_{1-x})_4O_9$ mixed crystals. Doped [5] and pure [6] $Bi_2Al_4O_9$ samples were prepared by the combustion synthesis route using the glycinenitrate process and followed by sintering at 1050–1090 °C. In another synthesis of $Bi_2Al_4O_9$ powders, annealing temperatures of 1000 °C were used [17]. $Bi_2Fe_4O_9$ was prepared at temperatures in the range 850–950 °C [7,18]. More recently, we applied the combined mechanochemical/thermal synthesis route in the preparation of $Bi_2(Fe_xAl_{1-x})_4O_9$ solid solutions; the desired phases were obtained after annealing the pre-activated $Bi_2O_3/Fe_2O_3/Al_2O_3$ mixtures at 800 °C for 24 h [19]. Thus, it is clearly demonstrated that mechanical pre-treatment of the reaction precursors has a positive effect on both temperature and duration of the subsequent thermal processing needed for the complete formation of $Bi_2M_4O_9$-type compounds. This is a result of the generally well-known phenomenon of *mechanical activation*, which has been applied to initiate or accelerate various chemical reactions [20–26]. In the present case, an enhanced high-temperature reactivity of the mechanically activated $Bi_2O_3/Ga_2O_3/Al_2O_3$ mixtures is a result of complex structural changes in the oxides due to the mechanically induced defects. Obviously, the nanoscale nature of the mechanically activated oxide precursors revealed by XRD, and consequently their large surface area and larger contacts between them, play an essential role in the subsequent thermal process. The reduction of the sintering temperature and the shortening of the reaction time needed for the complete formation of the desired $Bi_2(Ga_xAl_{1-x})_4O_9$ compounds can be understood as a result of an accelerated mass transfer and an enhanced ionic diffusivity at contacts zones between the precursors due to reduced diffusion paths in their nanostructures.

The XRD patterns of the selected as-prepared $Bi_2(Ga_xAl_{1-x})_4O_9$ solid solutions ($0 \le x \le 1$), shown in Fig. 2a, demonstrate that, with increasing gallium concentration ($x$), all the diffraction peaks shift towards lower $2\theta$ values. In addition, the intensity of some XRD peaks (e.g., peak corresponding to (0 0 1) plane) decreases,

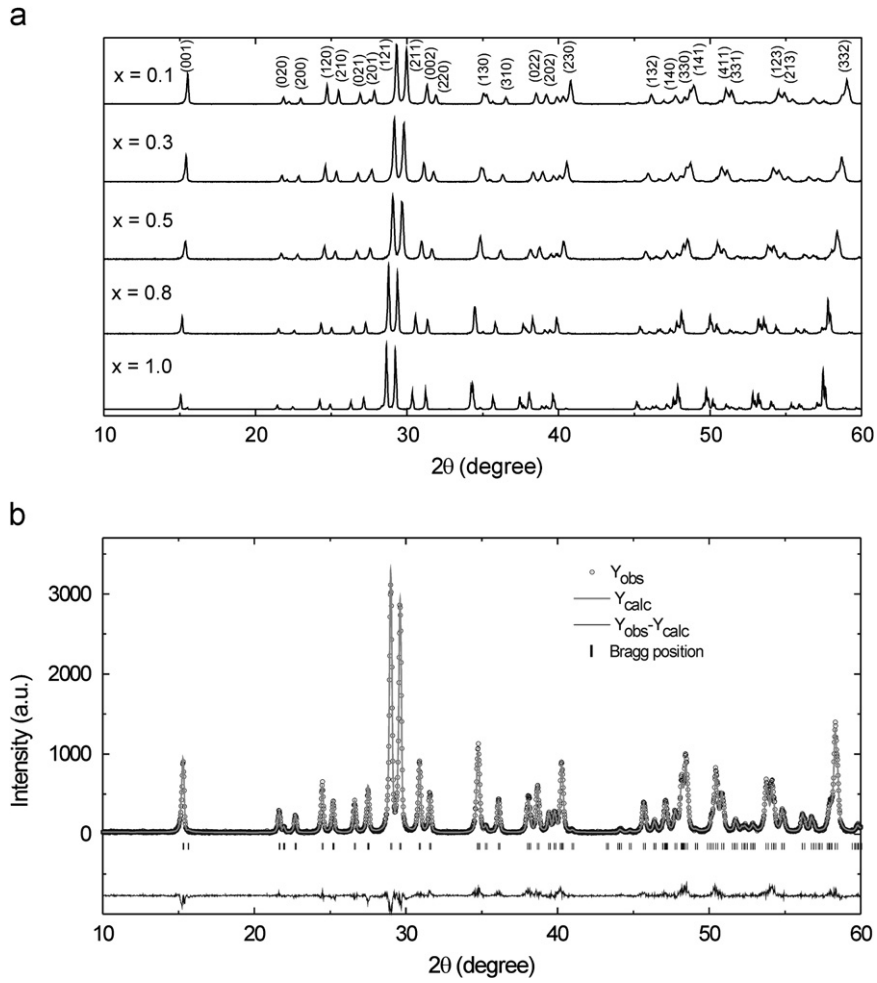


**Fig. 2.** (a) XRD patterns of selected $Bi_2(Ga_xAl_{1-x})_4O_9$ solid solutions prepared by the mechanochemical/thermal synthesis route and (b) the Rietveld refinement of the XRD data of the $Bi_2Ga_2Al_2O_9$ solid solution ($x=0.5$).

whereas the intensity of some peaks (e.g. (1 3 0)) increases with increasing $x$. This reflects both, the expansion of the crystal lattice and the redistribution of Ga and Al cations between ($T$) and [$O$] sites in the mullite-type materials with increasing $x$. To quantify these changes, the structure of the as-prepared $Bi_2(Ga_xAl_{1-x})_4O_9$ solid solutions was refined using the Rietveld method. The representative Rietveld refinement of the XRD data for the solid solution with $x=0.5$ is shown in Fig. 2b. Here, the solid curve represents the fit according to the refinement. The open circles are the observed XRD data and at the bottom, the difference between observed and calculated intensities is shown. Information on the Rietveld refinement of Fig. 2b and the corresponding crystallographic data are shown in Table 1. The Rietveld analysis reveals that the lattice parameters of the $Bi_2(Ga_xAl_{1-x})_4O_9$ solid solutions increase linearly with increasing gallium concentration, as expected according to Vegard's law (Fig. 3). Based on the analysis, the concentration-dependent lattice constants (in Å) and the volume of the unit cell (in Å$^3$) of the orthorhombic solid solutions can be expressed as follows: $a=7.719(2)+0.207(3)x$, $b=8.115(2)+0.184(4)x$, $c=5.687(3)+0.202(4)x$ and $V=356.1(3)+31.2(5)x$. These lattice parameters are in good agreement with the ones reported in the work of Debnath et al. [13,14] with deviations for $a$, $b$ and $c$ usually well below 1 pm. The crystallographic data and the goodness parameters of the fits resulting from the Rietveld analysis of the $Bi_2(Ga_xAl_{1-x})_4O_9$ solid solutions ($0\le x\le 1$) are listed in Table 2.

By means of Rietveld refinements, also the population of the different coordination sites has been derived. The analysis shows that gallium and aluminium cations are non-randomly distributed over the cation sites of octahedral and tetrahedral coordination. Whereas gallium ions preferably occupy tetrahedral sites, aluminium cations show an occupational preference for sites of octahedral coordination in the mullite-type structure of the

**Table 1**
Crystal structure parameters of $Bi_2Ga_2Al_2O_9$.

| | | | |
|---|---|---|---|
| Empirical formula | $Bi_2Ga_2Al_2O_9$ | | |
| Crystal system | Orthorhombic | | |
| Space group | *Pbam* (No. 55) | | |
| $a$ (Å) | 7.82715(34) | | |
| $b$ (Å) | 8.20793(38) | | |
| $c$ (Å) | 5.78675(27) | | |
| V (Å$^3$) | 371.769(29) | | |
| Atomic positions | $x$ | $y$ | $z$ |
| Bi-4$g$ | 0.1714(2) | 0.1679(2) | 0.0000(0) |
| $Ga_1$-4$f$ | 0.5000(0) | 0.0000(0) | 0.2638(1) |
| $Ga_2$-4$h$ | 0.3522(5) | 0.3384(7) | 0.5000(0) |
| $Al_1$-4$f$ | 0.5000(0) | 0.0000(0) | 0.2638(1) |
| $Al_2$-4$h$ | 0.3522(5) | 0.3384(7) | 0.5000(0) |
| $O_1$-2$b$ | 0.0000(0) | 0.0000(0) | 0.5000(0) |
| $O_2$-8$i$ | 0.6227(1) | 0.7872(1) | 0.2608(2) |
| $O_3$-4$g$ | 0.1373(2) | 0.4152(2) | 0.5000(0) |
| $O_4$-4$h$ | 0.1463(2) | 0.4410(2) | 0.0000(0) |
| $R$-values (%) | $R_p=9.16$, | $R_{wp}=12.3$, | $R_{exp}=8.39$ |

$Bi_2(Ga_xAl_{1-x})_4O_9$ solid solutions. This preference of gallium for the tetrahedrally coordinated sites has already been observed by Giaquinta et al. [3] in the case of $Bi_2(Fe_xGa_{1-x})_4O_9$ and also by Debnath et al. [13,14] in the case of $Bi_2(Ga_xAl_{1-x})_4O_9$. Fig. 4 shows the site occupancies, $f(i_\alpha)=N(i_\alpha)/2$, of Al and Ga in the tetrahedral and octahedral sites, derived from the Rietveld analysis, where $N(i_\alpha)$ denotes the number of cations of type $i$ ($i$=Ga, Al) on sites of type $\alpha$ ($\alpha=(T)$, $[O]$) per formula unit of $Bi_2M_4O_9$, $M$=Ga, Al. In the graph, the random distribution of the $M^{3+}$ cations is indicated by the dashed diagonal lines. In order to emphasize more clearly the deviation from the random solid solution, Fig. 5 shows occupation probabilities of the cations, $\lambda(i_\alpha)$, given by the fraction of cations of type $i$ located on sites of type $\alpha$, $\lambda(i_\alpha)=N(i_\alpha)/(N(i_{(T)})+N(i_{[O]}))$. In this figure, the random case is given by the horizontal dashed line at $\lambda(i_\alpha)=0.5$. As seen, for small contents of Al (Ga) the probability that an aluminium (gallium) ion is located on an octahedral (tetrahedral) site amounts up to 80%. Quantitative information on the cation distribution for the whole range of the solid solutions is listed in Table 3.

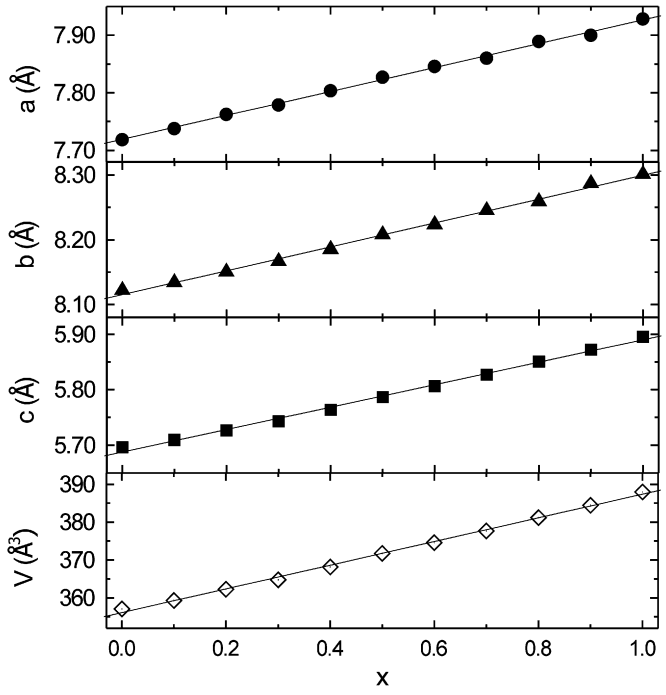


**Fig. 3.** Structural parameters of $Bi_2(Ga_xAl_{1-x})_4O_9$ solid solutions. The solid lines represent the behaviour expected according to Vegard's law.

The EDX analysis of the as-prepared $Bi_2(Ga_xAl_{1-x})_4O_9$ solid solutions confirmed the presence of only the constituent elements Bi, Ga, Al, and O and indicated that there is no contamination of the reaction products from the tungsten carbide chamber and balls used in the combined mechanochemical/thermal synthesis; see the representative EDX spectrum in Fig. 6. In addition, the average atomic concentrations of bismuth, gallium, aluminium, and oxygen were found to be in good agreement with the stoichiometric formula of the as-prepared $Bi_2(Ga_xAl_{1-x})_4O_9$ solid solutions.

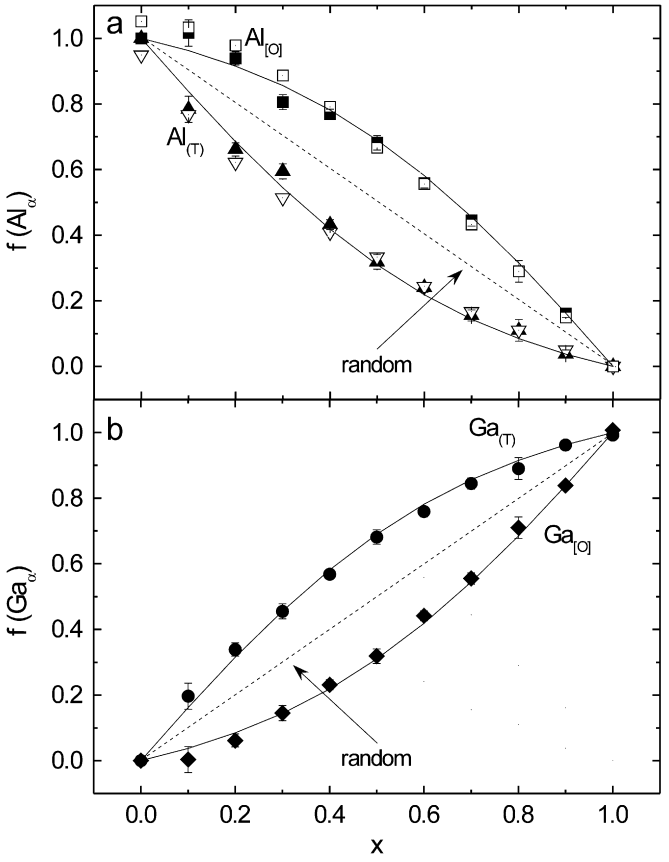


**Fig. 4.** Fractions, $f(i_\alpha)=N(i_\alpha)/2$, of tetrahedral and octahedral sites occupied by (a) Al and (b) Ga in the $Bi_2(Ga_xAl_{1-x})_4O_9$ series obtained from Rietveld refinement of XRD data (full symbols) and fractions of sites occupied by Al as derived from $^{27}$Al MAS NMR (open symbols). The random distribution is indicated by the dashed diagonal lines. The full lines represent fits to the experimental data according to Eq. (2) with $K_D=0.201$, see text.

**Table 2**
Lattice constants ($a$, $b$, and $c$), volume of unit cell ($V$) and the goodness parameters of the fits ($R_p$, $R_{wp}$, $R_{exp}$, $\chi^2$, and $S$) resulting from the Rietveld analysis of the $Bi_2(Ga_xAl_{1-x})_4O_9$ solid solutions ($0 \le x \le 1$).

| $x$ | $a$ (Å) | $b$ (Å) | $c$ (Å) | $V$ (Å$^3$) | $R_p$ (%) | $R_{wp}$ (%) | $R_{exp}$ (%) | $\chi^2$ | $S$[a] |
|---|---|---|---|---|---|---|---|---|---|
| 0 | 7.71875(29) | 8.12195(31) | 5.69640(21) | 357.114(23) | 8.28 | 11.3 | 6.14 | 3.41 | 1.84 |
| 0.1 | 7.73775(36) | 8.13378(40) | 5.70942(28) | 359.334(30) | 8.36 | 11.1 | 5.64 | 3.91 | 1.97 |
| 0.2 | 7.76256(33) | 8.15027(36) | 5.72671(25) | 362.312(28) | 7.88 | 10.9 | 5.52 | 3.93 | 1.97 |
| 0.3 | 7.77905(40) | 8.16636(45) | 5.74308(31) | 364.806(38) | 8.08 | 11.1 | 5.55 | 4.01 | 2.00 |
| 0.4 | 7.80345(33) | 8.18522(36) | 5.76382(25) | 368.152(28) | 7.18 | 9.85 | 5.51 | 3.20 | 1.79 |
| 0.5 | 7.82715(34) | 8.20793(38) | 5.78675(27) | 371.769(29) | 9.16 | 12.3 | 8.39 | 2.17 | 1.47 |
| 0.6 | 7.84584(30) | 8.22344(33) | 5.80619(22) | 374.614(25) | 7.14 | 9.76 | 5.44 | 3.22 | 1.79 |
| 0.7 | 7.86028(24) | 8.24509(26) | 5.82713(18) | 377.655(20) | 7.22 | 10.3 | 5.52 | 3.50 | 1.87 |
| 0.8 | 7.88949(16) | 8.25908(17) | 5.85041(12) | 381.213(13) | 8.42 | 10.9 | 5.52 | 3.86 | 1.97 |
| 0.9 | 7.90025(24) | 8.28694(26) | 5.87204(17) | 384.436(20) | 6.99 | 9.48 | 5.43 | 3.05 | 1.75 |
| 1.0 | 7.92859(15) | 8.30125(16) | 5.89515(11) | 388.002(13) | 8.71 | 11.4 | 5.69 | 4.03 | 2.00 |

[a] $S=R_{wp}/R_{exp}$.

To determine the cation distribution in the $Bi_2(Ga_xAl_{1-x})_4O_9$ mixed crystals by an independently supporting method, their local structure was also studied by high-resolution $^{27}Al$ MAS NMR. The NMR spectra for the solid solutions are shown in Fig. 7. It demonstrates very clearly the presence of two coordination sites for aluminium in the mullite-type structure; see the two well-resolved peaks in the region characteristic of tetrahedrally coordinated $Al^{3+}$ ions (chemical shift $\delta \approx 51$ ppm) and of octahedrally coordinated $Al^{3+}$ ($\delta \approx 10$ ppm). It is also visible that aluminium cations show an occupational preference for sites of octahedral coordination in the mullite-type structure of the $Bi_2(Ga_xAl_{1-x})_4O_9$ solid solutions. Moreover, this occupational preference is more pronounced for larger $x$; see the decreasing subspectral area ratio $A_{(T)}/A_{[O]}$ with increasing $x$ in Fig. 7. As can be recognized from Figs. 4a, 5a and Table 3, which contains also quantitative results from MAS NMR, excellent agreement is reached between the two sets of results obtained by the two different experimental techniques.

The distribution of the cations between the ($T$) and [$O$] sites in the mullite-type structure is determined by the homogeneous site exchange reaction of the $M^{3+}$ cations

$$Al_{(T)} + Ga_{[O]} \rightleftarrows Al_{[O]} + Ga_{(T)} \quad (1)$$

where, $Al_{(T)}$ ($Ga_{(T)}$) and $Al_{[O]}$ ($Ga_{[O]}$) denote aluminium (gallium) ions on tetrahedrally and octahedrally coordinated sites, respectively. At thermodynamic equilibrium this defines the cation distribution coefficient $K_D$ given by Eq. (2) following the mass action law

$$K_D = \frac{N(Al_{(T)})\,N(Ga_{[O]})}{N(Al_{[O]})\,N(Ga_{(T)})} \quad (2)$$

In the case of a random distribution of cations, $K_D$ takes the value of unity. In the present case, the distribution coefficient assumes a value of about 0.2, see Table 3 and the fits shown in Figs. 4 and 5. The latter fits have been obtained by applying to Eq. (2) the conditions of site and atom conservation as well as the assumption that concentrations of vacancies on tetrahedral and octahedral sites are always negligible in comparison to the

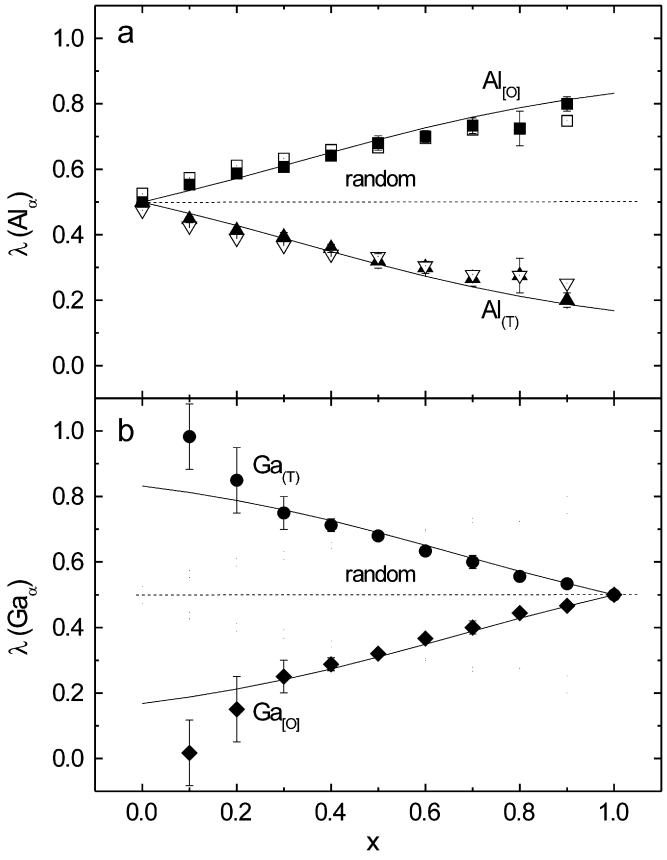


**Fig. 5.** Fractions, $\lambda(i_\alpha)=N(i_\alpha)/(N(i_{(T)})+N(i_{[O]}))$, of (a) Al and (b) Ga cations on sites of type $\alpha$ ($\alpha=(T)$, $[O]$) in the $Bi_2(Ga_xAl_{1-x})_4O_9$ solid solutions. The random distribution is indicated by the dashed horizontal lines. The full lines represent fits to the experimental data according to Eq. (2) with $K_D=0.201$, see text.

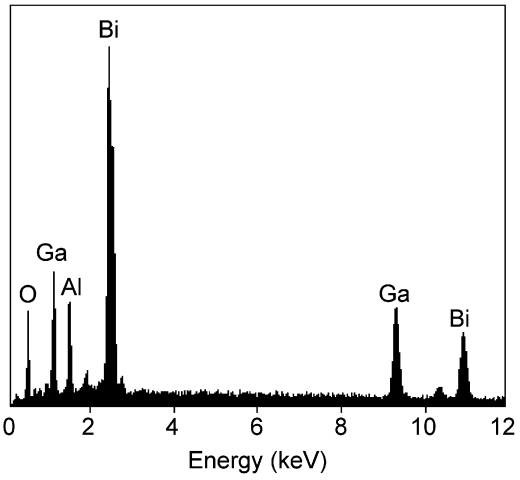


**Fig. 6.** EDX spectrum of the $Bi_2Ga_2Al_2O_9$ solid solution ($x=0.5$).

**Table 3**
Cation distribution in the $Bi_2(Ga_xAl_{1-x})_4O_9$ solid solutions. To emphasize the site occupancy at the atomic level, the structural formula of the solid solutions is formulated as $Bi_2(Ga, Al)_2[Ga, Al]_2O_9$, where round and square brackets enclose both $Ga^{3+}$ and $Al^{3+}$ cations on sites of tetrahedral and octahedral coordination, respectively. At thermodynamic equilibrium the cation distribution is defined by the coefficient $K_D$ given by Eq. (2).

| $x$ | Cation distribution derived from Rietveld refinements (XRD) | Cation distribution derived from NMR | $K_D$[a] |
|---|---|---|---|
| 0 | $Bi_2(Al)_2[Al]_2O_9$ | $Bi_2(Al_{0.47})_2[Al_{0.53}]_2O_9$ | – |
| 0.1 | $Bi_2(Ga_{0.20}Al_{0.80})_2[Ga_{0.00}Al_{1.00}]_2O_9$ | $Bi_2(Ga_{0.20}Al_{0.80})_2[Ga_{0.00}Al_{1.00}]_2O_9$ | 0.01 |
| 0.2 | $Bi_2(Ga_{0.34}Al_{0.66})_2[Ga_{0.06}Al_{0.94}]_2O_9$ | $Bi_2(Ga_{0.38}Al_{0.62})_2[Ga_{0.02}Al_{0.98}]_2O_9$ | 0.12 |
| 0.3 | $Bi_2(Ga_{0.45}Al_{0.55})_2[Ga_{0.15}Al_{0.85}]_2O_9$ | $Bi_2(Ga_{0.49}Al_{0.51})_2[Ga_{0.11}Al_{0.89}]_2O_9$ | 0.22 |
| 0.4 | $Bi_2(Ga_{0.57}Al_{0.43})_2[Ga_{0.23}Al_{0.77}]_2O_9$ | $Bi_2(Ga_{0.59}Al_{0.41})_2[Ga_{0.21}Al_{0.79}]_2O_9$ | 0.22 |
| 0.5 | $Bi_2(Ga_{0.68}Al_{0.32})_2[Ga_{0.32}Al_{0.68}]_2O_9$ | $Bi_2(Ga_{0.72}Al_{0.28})_2[Ga_{0.28}Al_{0.72}]_2O_9$ | 0.22 |
| 0.6 | $Bi_2(Ga_{0.76}Al_{0.24})_2[Ga_{0.44}Al_{0.56}]_2O_9$ | $Bi_2(Ga_{0.76}Al_{0.24})_2[Ga_{0.44}Al_{0.56}]_2O_9$ | 0.25 |
| 0.7 | $Bi_2(Ga_{0.84}Al_{0.16})_2[Ga_{0.56}Al_{0.44}]_2O_9$ | $Bi_2(Ga_{0.83}Al_{0.17})_2[Ga_{0.57}Al_{0.43}]_2O_9$ | 0.24 |
| 0.8 | $Bi_2(Ga_{0.89}Al_{0.11})_2[Ga_{0.71}Al_{0.29}]_2O_9$ | $Bi_2(Ga_{0.89}Al_{0.11})_2[Ga_{0.71}Al_{0.29}]_2O_9$ | 0.30 |
| 0.9 | $Bi_2(Ga_{0.96}Al_{0.04})_2[Ga_{0.84}Al_{0.16}]_2O_9$ | $Bi_2(Ga_{0.95}Al_{0.05})_2[Ga_{0.85}Al_{0.15}]_2O_9$ | 0.22 |
| 1.0 | $Bi_2(Ga)_2[Ga]_2O_9$ | $Bi_2(Ga)_2[Ga]_2O_9$ | – |

[a] Calculated on the basis of XRD data.

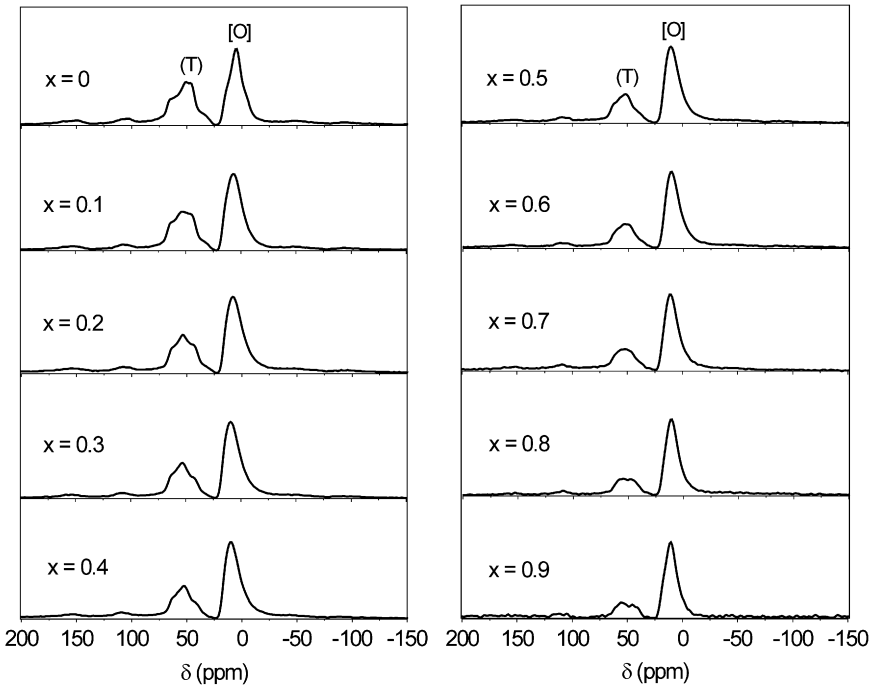


**Fig. 7.** $^{27}$Al MAS NMR spectra of $Bi_2(Ga_xAl_{1-x})_4O_9$ solid solutions.

concentrations of $M^{3+}$ cations on these sites. As seen in Figs. 4 and 5, the values calculated for site and cation fractions fit the experimental data quite well. Only for $x=0.1$, the experimental fractions of gallium ions occupying the two structural sites deviates significantly, Fig. 5b. In part, however, this may be due to error propagation which causes large errors for the minority component as indicated by the error bars in Fig. 5b for small gallium contents. The $K_D$ value of about 0.2 gives further clear evidence of a cation distribution that is far from random in the whole series of solid solutions. It is interesting to note that the data of Debnath et al. [13,14] indicate a cation distribution coefficient of about 0.5. It remains open at present whether this significant difference is due to the different synthesis routes employed.

In conclusion, the present work on $Bi_2(Ga_xAl_{1-x})_4O_9$ solid solutions gives clear evidence of a considerable deviation of the cation distribution from the random distribution ($\lambda=0.5$, Fig. 5). Results derived from Rietveld refinement of XRD data and from the nuclear spectroscopic method are in good agreement for the whole series of solid solutions, see Figs. 4, 5 and Table 3. Both experimental techniques reveal the occupational preference of gallium cations for tetrahedral sites. This preference may be explained by the ability of gallium ions to form bonds of more covalent character at these sites than aluminium ions can do. As convincingly demonstrated by Figs. 4, 5 and Table 3, this preference leads to a far from random distribution of cations across the whole series of $Bi_2(Ga_xAl_{1-x})_4O_9$ solid solutions.

## 4. Conclusions

For the first time, complex mullite-type $Bi_2(Ga_xAl_{1-x})_4O_9$ solid solutions with $0 \le x \le 1$ have been synthesized via high-energy ball milling of stoichiometric $Bi_2O_3/Ga_2O_3/Al_2O_3$ mixtures followed by subsequent annealing at 800 °C for 24 h. EDX analysis proved that there is no contamination by tungsten carbide from the milling process. Compared with other synthesis routes, the combined mechanochemical/thermal synthesis of the pure $Bi_2(Ga_xAl_{1-x})_4O_9$ solid solutions represents a simple, less elaborate, high-yield, lower temperature, and faster procedure for the synthesis of bismuth-bearing oxides with the mullite structure. The as-prepared mullites have been investigated by XRD and $^{27}$Al MAS NMR. The orthorhombic structure of the $Bi_2(Ga_xAl_{1-x})_4O_9$ solid solutions was resolved and determined to be isostructural with that of the end members $Bi_2Ga_4O_9$ and $Bi_2Al_4O_9$. The lattice parameters of the $Bi_2(Ga_xAl_{1-x})_4O_9$ mixed crystals were found to vary linearly with gallium content and they change in accordance with Vegard's law. The Rietveld refinements of the XRD data as well as the analysis of the NMR spectra have clearly revealed the preference of $Ga^{3+}$ cations for tetrahedral sites and of $Al^{3+}$ for octahedral sites, leading to a significantly non-random distribution of cations in the whole series of the $Bi_2(Ga_xAl_{1-x})_4O_9$ mullite-type solid solutions.

## Acknowledgment

The authors thank the DFG (SPP 1415) for support of the present work. Partial support by the VEGA (2/0174/11) is gratefully acknowledged.

## References

[1] R.X. Fischer, H. Schneider, Mullite, in: H. Schneider, S. Komarneni (Eds.), Wiley-VCH, Weinheim, 2005, pp. 1–140.
[2] J. Schreuer, M. Burianek, M. Mühlberg, B. Winkler, D.J. Wilson, H. Schneider, J. Phys.: Condens. Matter 18 (2006) 10977–10988.
[3] D.M. Giaquinta, G.C. Papaefthymiou, W.M. Davis, H.-C. zur Loye, J. Solid State Chem. 99 (1992) 120–133.
[4] D.M. Giaquinta, G.C. Papaefthymiou, H.-C. zur Loye, J. Solid State Chem. 114 (1995) 199–205.
[5] S. Zha, J. Cheng, Y. Liu, X. Liu, G. Meng, Solid State Ionics 156 (2003) 197–200.
[6] I. Bloom, M.C. Hash, J.P. Zebrowski, K.M. Myles, M. Krumpelt, Solid State Ionics 53-56 (1992) 739–747.
[7] I. Abrahams, A.J. Bush, G.E. Hawkes, T. Nunes, J. Solid State Chem. 147 (1999) 631–636.
[8] J.B. Goodenough, Ann. Rev. Mater. Res. 33 (2003) 91–128.
[9] G. Blasse, O.B. Ho, J. Lumin. 21 (1980) 165–168.
[10] V.V. Volkov, A.V. Egorysheva, Opt. Mater. 5 (1996) 273–277.

[11] L. López-de-la-Torre, A. Friedrich, E.A. Juarez-Arellano, B. Winkler, D.J. Wilson, L. Bayarjargal, M. Hanfland, M. Burianek, M. Mühlberg, H. Schneider, J. Solid State Chem. 182 (2009) 767–777.
[12] F.J. Palomares, E. Paz, F. Soria, J.S. Moya, M. Burianek, M. Muehlberg, H. Schneider, J. Am. Ceram. Soc. 92 (2009) 2993–2998.
[13] T. Debnath, C.H. Rüscher, P. Fielitz, S. Ohmann, G. Borchardt, Ceram. Trans. 217 (2010) 71–78.
[14] T. Debnath, C.H. Rüscher, P. Fielitz, S. Ohmann, G. Borchardt, J. Solid, State Chem. 183 (2010) 2582–2588.
[15] J. Rodriguez-Carvajal, Fullprof Program, version 2.4.2, ILL Grenoble, Grenoble, France, 1993.
[16] D. Voll, A. Beran, H. Schneider, Phys. Chem. Miner. 33 (2006) 623–628.
[17] R. Arpe, H.K. Müller-Buschbaum, J. Inorg. Nucl. Chem. 39 (1977) 233–235.
[18] A.S. Poghossian, H.V. Abovian, P.B. Avakian, S.H. Mkrtchian, V.M. Haroutunian, Sensor. Actuat. B—Chem. 4 (1991) 545–549.
[19] K.L. Da Silva, V. Šepelák, A. Paesano Jr., F.J. Litterst, K.D. Becker, Z. Anorg. Allg. Chem. 636 (2010) 1018–1025.
[20] V.V. Boldyrev, Russ. Chem. Rev. 75 (2006) 177–189.
[21] G. Heinicke, Tribochemistry, Akademie-Verlag, Berlin, 1984.
[22] E. Avvakumov, M. Senna, N. Kosova, Soft Mechanochemical Synthesis: A Basis for New Chemical Technologies, Kluwer Academic Publishers, Boston, 2001.
[23] M.K. Beyer, H. Clausen-Schaumann, Chem. Rev. 105 (2005) 2921–2948.
[24] J.D.E. White, R.V. Reeves, S.F. Son, A.S. Mukasyan, J. Phys. Chem. A 113 (2009) 13541–13547.
[25] G. Mulas, F. Delogu, S. Enzo, L. Schiffini, G. Cocco, J. Alloy. Compd. 483 (2009) 642–644.
[26] F. Delogu, G. Mulas, Experimental and Theoretical Studies in Modern Mechanochemistry, Transworld Research Network, Kerala, 2010.